ISIJ International, Vol. 42 (2002), No. 3, pp. 299–303

The Effect of Processing History on a Cold Rolled and Annealed Mo–Nb Microalloyed TRIP Steel

S. JIAO, F. HASSANI,[1)] R. L. DONABERGER,[2)] E. ESSADIQI[3)] and S. YUE[3)]

Department of Mining Metals and Materials Engineering, McGill University, 3610 University Street, Montreal, Quebec, H3A 2B2 Canada. 1) Formerly at McGill UIniversity. Now at Stelco, Inc., Hamilton, Ont., L8N 3T1 Canada.
2) Neutron Program for Materials Research, Chalk River Laboratories, Chalk River, ON, K0J 1J0 Canada.
3) CANMET-MTL, Ottawa, ON, K1A 0G1 Canada.

(*Received on August 13, 2001; accepted in final form on December 10, 2001*)

In this paper, a Mo–Nb microalloyed TRIP Steel was subjected to several heat treatments designed to generate different microstructures. These microstructures were then cold rolled and TRIP-annealed, and the resulting tensile properties and retained austenite characteristics were determined. The results reveal that prior heat treatment has a significant effect on the cold rolled and annealed behavior. Generally, an increasing volume fraction of proeutectoid ferrite prior to cold rolling and TRIP annealing leads to improved tensile ductility. This is due to increased work-hardening rates, which, in turn, correlate to increased carbon enrichment in the retained austenite. These results can clearly be used to optimize the hot rolling process to produce hot strip for the subsequent production of cold rolled Mo-Nb TRIP Steel.

KEY WORDS: Mo–Nb TRIP Steel; prior heat treatments; austenite retention; carbon enrichment.

1. Introduction

In cold rolled and annealed steels, such as Al-killed, deep drawing quality grades, the as-hot rolled structure has been found to be extremely important in controlling the Al precipitation, since this subsequently influences the development of the cold rolled and annealed texture. A study on cold drawn and annealed rod also revealed a significant effect of the hot rolling schedule on the behavior of the cold rolled and annealed product.[1)] Although much work has been generated on cold-rolled and annealed TRIP steels, little attention has been paid to the effect of prior hot rolling of these steels. This is because the subsequent processing after hot rolling appears to radically alter the microstructure, presumably much reducing any effect of the prior microstructure. In this paper, a Si–Mn TRIP steel microalloyed with Mo and Nb was subjected to heat treatments designed to create several different types of microstructure. These were then subjected to cold rolling and TRIP annealing, and the subsequent tensile properties and retained austenite characteristics were then determined.

2. Experimental

2.1. Chemical Composition

The Si–Mo–Nb steel studied in this work was produced and received in the as-hot rolled condition. The chemical composition is shown in **Table 1**. Nb in solid solution has been found to improve the TRIP properties[2)]; Mo retards the precipitation of Nb(C, N), thus potentially improving the effectiveness of Nb as a TRIP enhancer.[3)]

Table 1. Chemical composition (mass%).

C	Si	Mn	Nb	Mo	Al	N
0.2	1.55	1.55	0.035	0.3	0.028	0.006

2.2. Prior Heat Treatments

To generate the initial microstructures, specimens of rectangular cross-section, 20×5 mm, and 75 mm long were heat treated in a radiant furnace in an atmosphere of flowing Ar gas. The heat treatments, which are shown schematically in **Fig. 1**, are described as follows.

All samples were first soaked at 1 200°C for 30 min to dissolve any precipitates.

The SC (fast cooled) specimen was directly cooled down to ambient at a cooling rate of 1°C/s.

The PPT700 (precipitation and 700°C intercritical hold) heat treatment was cooled down first to 950°C at a cooling rate of 1°C/s and then held at this temperature for 30 min. The specimen was then cooled to the intercritical temperature of 700°C at the same cooling rate and held for 30 min. Finally, it was cooled down to room temperature at a rate of 0.5°C/s.

The FC700 (furnace cooled and held at 700°C) was the same as the PPT700, minus the 950°C segment.

The FC650A treatment was the same as the PPT700, but had a lower intercritical temperature and shorter time, *i.e.*, 650°C and 10 min instead of 700°C and 30 min.

FC650B was the same as FC650A, but the intercritical hold time was increased to 30 min.

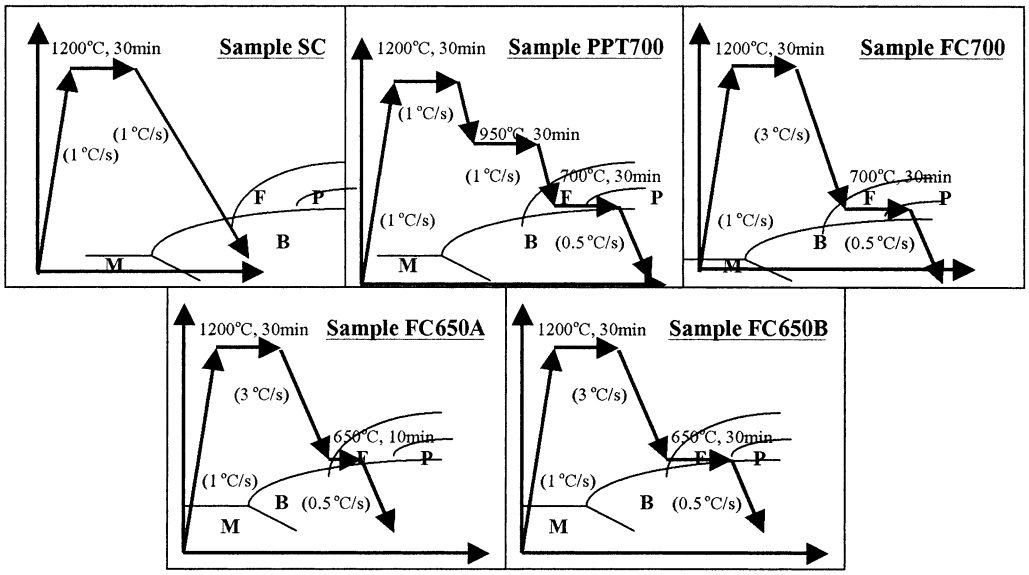

Fig. 1. Five prior heat treatment routes relative to the CCT.

2.3. Cold Rolling and Annealing

After mechanical descaling, samples from above heat treatments were cold rolled on a laboratory two-high rolling mill by 80% (*i.e.* sample thickness was reduced from 5 to 1 mm). As shown in **Fig. 2**, a conventional annealing process of TRIP steels was conducted in two salt baths to accommodate the 2 stages: (i) intercritical annnealing to produce some austenite and (ii) bainite transformation to retain some austenite down to room temperature. Microstructures of the prior and cold rolled and annealed structures were revealed in the normal manner, and some transmission electron microscopy of replicas was also performed.

2.4. Tensile Test

ASTM subsize E 8M-91 rectangular tensile specimen (6 mm in width and 25 mm in gauge length) were machined from the cold rolled bands and were tested in a computerized servo-hydraulic test machine (MTS) at a crosshead speed of 0.01 mm/s for a strain rate of $4\times10\,s^{-1}$.

2.5. Retained Austenite Measurement

The volume fraction of retained austenite and the carbon concentration in the retained austenite were measured by neutron diffractometry (DUALSPEC powder diffractometer). The details of the test procedure are described elsewhere.[2,3)]

To determine the carbon concentration in the retained austenite, the austenite lattice parameter extrapolation method was used according to the following empirical expression[4)]:

$$a_O = 3.578 + 0.044\%C \quad \text{.....(1)}$$

3. Results

3.1. Microstructures after Prior Heat Treatments

The microstructures due to the prior heat treatments are all shown in **Fig. 3**. The main difference illustrated in these micrographs is a variation in the respective volume fractions of bainite and proeutectoid ferrite. As is expected, at 650°C, longer times led to increased levels of proeutectoid

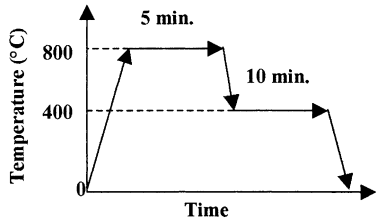

Fig. 2. Thermal cycles of the intercritical annealing.

ferrite. For this particular steel, increasing the intercritical temperature from 650 to 700°C also considerably increased the amount of proeutectoid ferrite for the same hold time. As may be expected, the volume fractions of bainite are similar for the FC700 and PPT700, since the intercritical segment was the same. However, the FC700 microstructure is coarser. This may be a result of the 950°C hold segment producing more precipitates, thereby inhibiting grain coarsening. The TEM replicas appear to support this hypothesis, as seen in **Fig. 4**.

The optical microstructures after cold rolling and TRIP annealing appeared to be independent of the prior heat treatment. A typical example is shown in **Fig. 5**. Compared to the prior microstructures, cold rolling and TRIP annealing has produced a much finer, more homogenous structure comprising of an equiaxed ferrite and an unresolvable bainite/retained austenite second phase.

3.2. Tensile Test Curves and Mechanical Properties

The true tensile strain–stress curves (up to the maximum stress) from tensile test of the samples after intercritical annealing are displayed in **Fig. 6**. As well, the mechanical properties are summarized in **Table 2**. In general, the specimens that had prior microstructures that were predominantly bainitic (SC and 650A) had significantly inferior ductility. Comparing these two with each other, the SC structure, which had a prior structure that was almost completely bainitic, exhibited a much higher strength, but a slightly inferior ductility. All the other structures (PPT700, FC700 and 650B) had quite similar ductility. Of these three, the

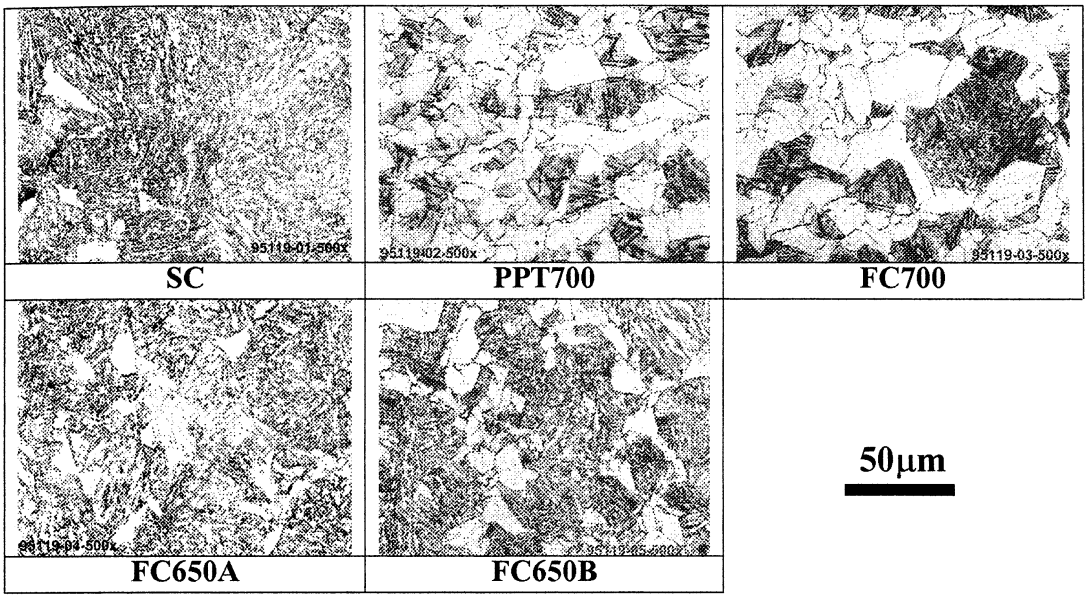

Fig. 3. Optical micrographs delivered after different prior heat treatments.

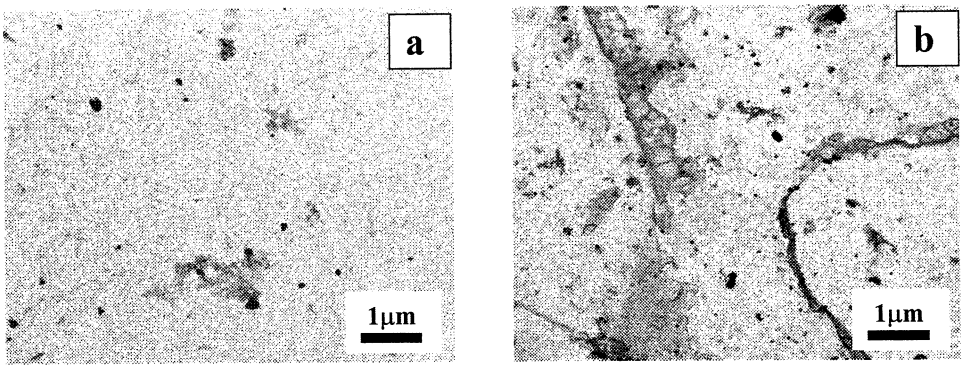

Fig. 4. TEM bright micrographs showing the morphology of precipitations. (a): PPT700 and (b): FC700

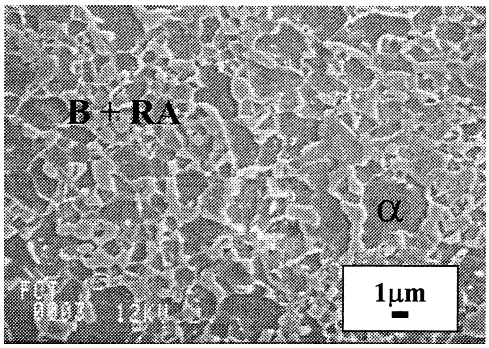

Fig. 5. SEM micrograph of SC sample delivered after the intercritical annealing.

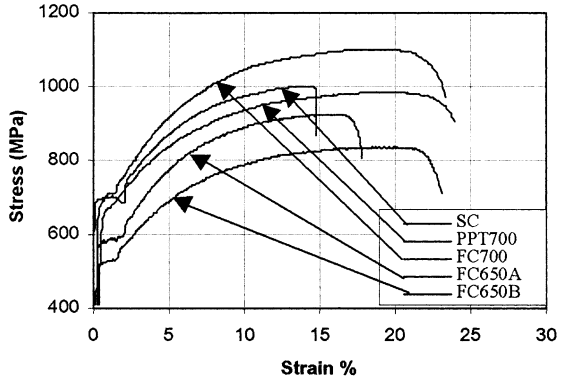

Fig. 6. True strain–stress curves of tensile test for the samples after the intercritical annealing.

two with higher fraction of prior proeutectoid ferrite (PPT700, FC700) exhibited much superior strengths (indeed, the 650B structure had the lowest strength of all 5 structures). The FC700 exhibited the best strength of all the structures tested.

3.3. Retained Austenite and Its Carbon Concentration

The retained austenite volume fractions and carbon concentrations are illustrated in **Fig. 7**. The retained austenite

Table 2. Mechanical properties.

Route	YS(MPa)	UTS(MPa)	U·EL (%)	EL (%)	n	UTSxEL
SC	695	1002	14.1	14.9	0.13	14128.2
PPT700	660	986	19.1	23.9	0.18	23565.4
FC700	710	1102	19.1	23.4	0.18	25786.8
FC650A	592	926	15.7	17.8	0.15	16482.8
FC650B	520	836	19.7	23.1	0.18	19311.6

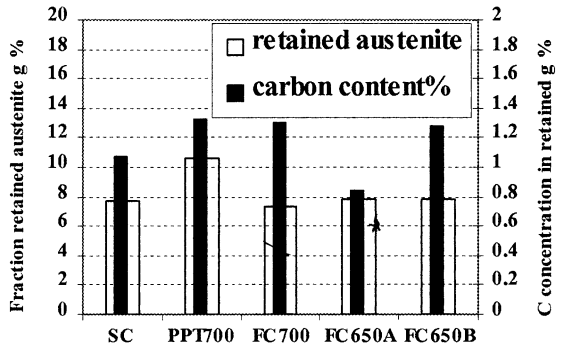

Fig. 7. Fraction retained austenite and its carbon concentration.

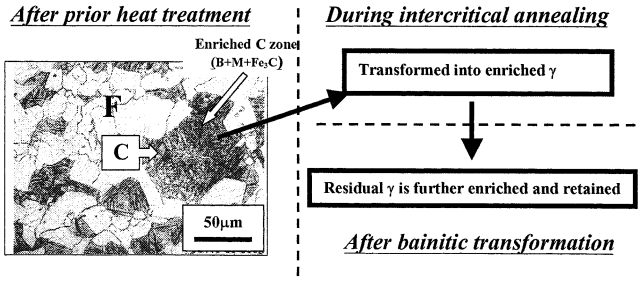

Fig. 8. Schematic illustration of carbon enrichment in retained austenite during the whole experiment process.

volume fractions are all similar, with the exception of PPT700, which possesses a slightly higher value. The retained austenite carbon concentrations exhibit slightly more variability, but in general can classified into 2 groups, a higher concentration group comprised of the specimens with superior ductility, and the others which exhibit both lower ductility and lower levels of carbon.

4. Discussion

4.1. Carbon Enrichment of the Retained Austenite

The variation in enrichment level of retained austenite for different samples is presumed to be due to the different proeutectoid ferrite volume fractions in the prior microstructures. There are actually four stages of carbon partitioning that take place in the whole processing history of these specimens. The first two occur in the prior heat treatment and other two take place during TRIP annealing. The first carbon partitioning event commenced with the start of austenite-to-ferrite transformation in the prior heat treatment. Due to the lower carbon solubility proeutectoid ferrite, carbon is rejected into the remaining austenite and enriches the untransformed austenite. Obviously, the more ferrite generated, the richer in carbon the remaining austenite becomes. The second carbon partitioning is achieved during the austenite-to-bainite transformation following the austenite-to-ferrite transformation in the prior heat treatment. During the bainitic transformation, some of the remaining austenite is transformed into bainite, further enriching the retained austenite, although some carbide precipitation may reduce this enrichment. As a consequence, after the prior heat treatment, the ferrite has little carbon, and the 'second phase' (comprising of bainite and possibly carbides, retained austenite and martensite) has a high carbon concentration, as is demonstrated in **Fig. 8**. During the

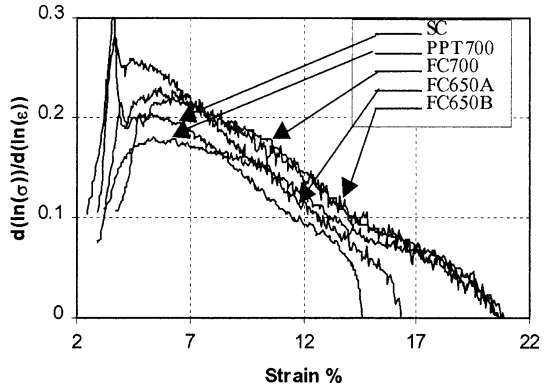

Fig. 9. The strain hardening behavior of the samples during tensile test.

intercritical annealing of the TRIP anneal, austenite first nucleates in the enriched 'second phase'. Thus, the newly formed austenite inherits the carbon level of the second phase. Then, during the bainitic transformation stage of the TRIP anneal, some of the high carbon austenite transforms back into bainite and leaves the remaining austenite, and the subsequent retained austenite, further enriched and stabilized. Such a mechanism can explain why PPT700, FC700 and FC650B show a higher level of carbon enrichment than SC and FC650A.

4.2. Relationship between the Retained Austenite and Mechanical Properties

The combined analysis of Fig. 6 and Table 2 clearly indicates that good mechanical properties do not always coincide with high fraction retained austenite. For instance, SC, FC700, FC650A and FC650B all show rather different mechanical properties despite possessing similar fractions of retained austenite. On the other hand, the variation of carbon concentration in retained austenite corresponds far better with the mechanical properties. To clarify the mechanism behind this behavior, the incremental work-hardening characteristics of these samples were determined. Using a simple power law (Hollomon) relationship between true stain and stress as per Eq. (2):

$$\sigma = A\varepsilon^n \quad \text{.....(2)}$$

where σ and ε are respectively the true stress and the true strain. n is the work-hardening exponent and A is a constant, then

$$n = d(\ln((\sigma))/d(\ln \varepsilon) \quad \text{.....(3)}$$

The data converted from true strain–stress curves in Fig. 6 are plotted in **Fig. 9**. It can be seen that n values of SC and FC650A increase very quickly to a maximum at the beginning of straining but beyond this strain level, it decays rapidly. By contrast, the n values of the other three samples rise and fall much more gradually. This gradual and sustained work hardening rate behavior is considered to be classic TRIP behavior. This phenomena was considered by Evans[5] to be related to the decomposition (strain induced transformation (SIT) of retained austenite to martensite) behavior of retained austenite during tensile deformation. A rapid variation of n is always associated with the rapid SIT of the retained austenite. The stability of retained austenite

increases with increasing retained austenite carbon concentration and decreasing retained austenite particle size. According to Honeycombe *et al*.,[6] carbon is the most influential alloying element for the retention of austenite. Carbon enlarges the γ-field in a phase diagram and promotes the formation of austenite over wider compositional limits. Moreover, It is also well known that higher carbon content lowers the Ms temperature.

According to Sakuma *et al*.,[7] the mechanical stabilization of the retained austenite by carbon enrichment is achieved by the intensified interference between carbon atoms and formation of martensite. During nucleation and growth of martensite, as a martensite plate begins to form, strain generates dislocations and a change in lattice parameters. Stabilization comes into effect when interstitial elements such as carbon diffuse to dislocations and inhibit their further growth. Furthermore, the pinning of the dislocations could interfere with the motion or rotation of martensite.

Although this explains the ductility behavior, the strength variation is more difficult to rationalize, suggesting that more characterization of the final structures is required. Nevertheless, some generalities can be made. For example, for the prior structures with similar ductility (PPT700, FC700 and 650B), the two with higher fraction of prior proeutectoid ferrite (PPT700, FC700) exhibited much superior strengths. This may be related to higher levels of tetragonality in the resulting strain induced martensite, resulting from the higher carbon concentration of the retained austenite due to the prior heat treatment. More work is required to thoroughly explain the strength behavior, however.

5. Conclusions

The prior heat treatment significantly affects the mechanical properties of a cold rolled and annealed Mo–Nb microalloyed TRIP Steel.

Generally, higher levels of proeutectoid ferrite formed during the prior heat treatment leads to increased ductility and formability index (UTSxEL). This is in turn related to a retained austenite that is more enriched with carbon, optimizing the stability of retained austenite against strain induced transformation to martensite.

The results indicate that optimization of the hot rolling process is required to produce an optimized cold rolled and annealed Mo-Nb TRIP steel.

Acknowledgements

The financial support received from the Canadian Steel Industry Research Association (CSIRA) is acknowledged with gratitude. We are also very grateful to Mr. Edwin Fernandez, Mr. Abdelbaset Elwazri and Mr. Hongtao Fei for their help in the experiment design and performance.

REFERENCES

1) T. M. Maccagno, S. Yue, J. J. Jonas and K. Dyck: *Metall. Trans. A*, **24A** (1993), 1589.
2) A. Zarei-Hanzaki, P. D. Hodgson and S. Yue: *Metall. Trans. A*, **28A** (1997), 2405.
3) M. Bouet, J. Root, E. Es-Sadiqi and S. Yue: *Mater. Sci. Forum*, **284** (1998), 319.
4) B. D. Cullity: Elements of X-ray Diffraction, 2nd Ed., Addison-Wesley Publishing Company, Inc., Philippines, (1978), 350.
5) P. J. Evans, L. K. Crawford and A. Jonas: *Ironmaking Steelmaking*, **24** (1997), 361.
6) R. W. K. Honeycombe: Steels: Microstructure and Properties, American Society of Metals, University of Cambridge, London, (1982), 55.
7) Y. Sakuma, D. K. Matlock and G. Krauss: *Metall. Trans. A*, **23A** (1992), 1233.